

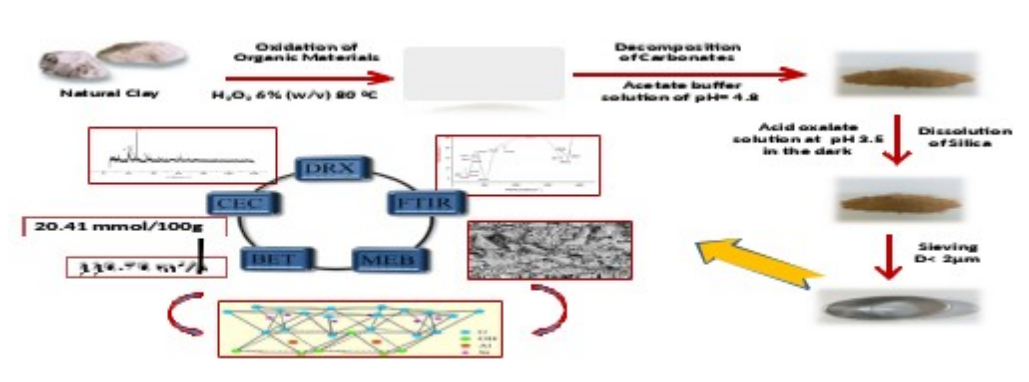
Physicochemical Characterization of Local clay from El-Oued Region, Southeastern of Algeria

Djamel Atia^a, Ammar Zobeidi^{*b}, Abasse Kamarchou^b, Salem Atia^b

^(a) Echahid Hama Lakhdar, El-Oued University. 39000 - Algeria

^(b) Pollution and waste treatment laboratory (PWTL), Kasdi Merbah Ouargla University .P.O. Box 511, 30000, Algeria.

Graphical abstract



Abstract

Keywords:
BET
clay minerals
El-Oued
FT-IR
SEM
XRD

The main purpose of the present study is the identification of the physico-chemical characteristics of local clay from a southeast province of Algeria (El Oued). A preliminary purification of organic compounds and calcite has been done in order to obtain granules with a diameter less than 2µm. Obtained granules were characterized by X-ray diffraction, FTIR, BET, SEM/EDS and CEC. X-ray diffraction shows a majority composition of illite, moderately of kaolinite and minority of quartz. FTIR showed the presence of all the characteristics peaks of the studied clay. The BET method reveals a specific area of about 110.786m²/g. SEM shows irregular shapes with ragged edges. EDS confirmed the results obtained by XRD. The value of CEC is about 20.416 mmol/100g.

1. Introduction

Clay refers to a naturally occurring material composed primarily of fine-grained minerals. The minerals found in clay are generally silicates less than 2 microns in size [1]. Clay is used as a rock term and as a particle-size term in the mechanical analysis of sedimentary rocks, soils, etc. As a rock term, it is difficult to define precisely, because of the wide variety of materials that have been called [2].

The first identification of a surface clay mineral is that it has a small grain size, generally $<2 \mu\text{m}$. Even if the reasons for the small crystal size, which are constantly observed are not fully understood at present, it is certainly the major characteristic of surface clay minerals [3].

However, the rapid change of mineralogy, on a geological scale at least, indicates subtle changes in the mineral structure as determined by X-ray diffraction, the major identification tool for clay minerals. Such change is the result of different chemical equilibrium [4].

The mineralogical and physico-chemical properties of clays are of particular interest in many applications such as water treatment, paint, the barrier for pollutants, adsorbent, catalyst, etc [5-7].

*Corresponding author.

E-mail address: zobeidi.aa@gmail.com (Ammar Zobeidi).

The interest given in recent years to the study of clays by numerous laboratories throughout the world is justified by their abundance in nature, their low cost, and the presence of electrical charges on their surfaces and, above all, the exchangeability of the interfoliar cations. All these properties make the clay a material of exceptional quality [8]. Several previous works worldwide have shown that clay minerals of smectite, montmorillonite, bentonite, illite, vermiculite, kaolinite or sepiolite have heavy metal adsorption capacities in effluents and waters contaminated.

Giving identification to new clay requires its characterization by several physicochemical methods (FTIR, XRD, SEM, BET, and CEC) to evaluate the potential of the studied clay to a very specific application (water treatment, etc.).

2. Materials and methods

2.1 Sampling region

The studied clay was harvested from "Sidi Omrane $33^{\circ}27'20''\text{N } 7^{\circ}11'0''\text{E}$ ", a commune located 137 km west of the capital of "El Oued" province and 210 km east of the capital of "Ouargla" province. The region of sampling is represented in Fig. 1 by a red circle.



Fig.1. Map of the sampling region

2.2. Preparation of a Sample of clay

Hydrogen peroxide (H_2O_2 6% w/v) was purchased from Kompass. Hydrochloric acid and sodium hexametaphosphate were purchased from Sigma Aldrich. The raw clay was preliminarily subjected to pre-sieving by a cascade of sieves in order to obtain sizes of less than 5 microns. Then it was gently crushed into powder and then treated with hydrogen peroxide (6% w/v) to remove organic compounds. A 2M hydrochloric acid solution was added then washed with distilled water several times to remove chloride and finally was dried at 105°C . Pipette method with the addition of a dispersible component (sodium hexa-metaphosphate) was used to obtain granules less than 2 microns. In order to confirm that all the granules size, a 2-micron electrospun sieve was used. The obtained granules were washed several times with bi-distilled water and by using the centrifuge to completely remove the chloride. The obtained powder was dried at 105°C [9].

2.3. X-ray fluorescence

X-ray diffraction (XRD) analysis was performed using automated (PAN analytical X'Pert-Pro) diffractometer equipment with $\text{CuK}\alpha 1$ radiation source with 1.540598 \AA of wavelength, at a step size angle of 0.02° , and a scan range from 5.053° to 120.046° .

2.4. Fourier-transform infrared spectroscopy

The study was carried out on a compacted clay pellet at a pressure of 80 kPa using a Shimadzu type IR AFFINITY-1 apparatus with a scan number equal to 8.

2.5. Brunauer-Emmett-Teller method (BET)

A sample of 0.2026 g was degassed at 100°C for 12 hours. The analysis was done with a Micromeritics ASAP 2020 V4.03 device with 77K liquid nitrogen.

2.6. Scanning Electron Microscope/EDS

Morphological, quantitative and qualitative analyses of the clay sample were carried out using SEM model JEOL 840.

2.7. Cation-exchange capacity (CEC)

The cation exchange capacity of the clay was determined by the Metson method [10]. The latter uses a clay mass $m = 10\text{g}$. The mass was coated with an ammonium acetate solution of 1 mol/L and then washed with isopropanol by filtration under vacuum and then finally washed with potassium chloride 1 mol/L solution to replace ammonium ions with potassium ions. The concentration of ammonium in the spray was measured using the chromatic method. The calculated concentration was about $C = 147 \text{ mg/L}$.

CEC was calculated according to the following relationship:

$$CEC (\text{mEq}/100 \text{ g}) = \frac{C * V * 100}{18 * m} \dots (1)$$

Where:

C: ammonium concentration (mg/L);

V: ammonium volume (L);

m: clay mass (g).

3. Results and discussion

3.1 XRD analysis

The diffraction pattern from XRD is shown in Fig 2. From the obtained figure it is observed that illite is the common major phase in the studied sample however, kaolinite and quartz are also present in minor quantity. To dissect the spectrum of DRX, software containing a large database called Match!V.2 was used. Table 1 summarizes the most intense peaks obtained by this software. The relatively high intensity of the quartz peaks in the WC clay (Fig 2) indicates a significant presence of the free silica.

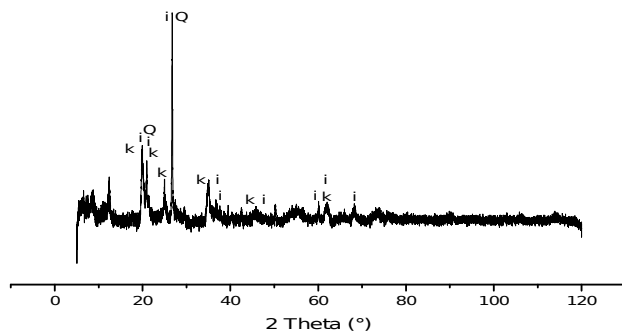


Fig. 2. X-ray diffraction FT-IR of studied clay.

3.1. Infrared Spectroscopy (FTIR) characterization

Infrared spectroscopy was used to complete the analysis of the clay sample and to reconfirm the results that were showed in X-ray Diffraction. The spectra obtained are illustrated in Fig 3. The OH stretching vibration bands at 3622.32 cm⁻¹, 3695.61 cm⁻¹, 1635.64 cm⁻¹, 798.53 cm⁻¹ indicate the presence of kaolinite. Nevertheless, at 3421.72 cm⁻¹ indicates the presence of water. However, OH stretching vibration band at 3552.88 cm⁻¹ indicates internal OH. The Si-O-Al stretching vibration bands at 428.2 cm⁻¹, 474.49 cm⁻¹, 752.24 cm⁻¹, 1033.85 cm⁻¹ show the presence of illite, while at 694.37 cm⁻¹ is an evidence of the presence of kaolinite. The Si-O-Si stretching vibration bands at 532.35 cm⁻¹ and 779.24 cm⁻¹ indicate the presence of quartz. The Al-O band at 1392.61 cm⁻¹ and the Al-OH stretching vibration band at 914.24 cm⁻¹ are also marks of the presence of illite. Table 2 resumes the principal peaks. It should be noted that a small, insignificant peak appears at about 2380.16 cm⁻¹ indicating the presence of a carbon from carbonate component in the sample.

Table1:

Qualitative analysis of the X-ray diffraction results of the studied clay sample

2θ (°)	d-spacing (Å)	Intensities	Phase	Reference
19.73	4.4952	271.69	Illite	[11]
19.92	4.4500	383.58		
20.68	4.2924	168.27		
26.62	3.3463	430.52		
19.85	4.4600	361.32	Kaolinite	[12]
20.34	4.3633	206.28		
20.45	4.3400	163.61		
24.86	3.5784	147.87		
34.97	2.5638	185.91		
35.09	2.5551	181.03		
20.9	4.2469	283.54		
26.69	3.3301	471.32		

Table 2:

FTIR bands of the natural clay

Absorptio (cm ⁻¹)	Molecular bond	Phase	Reference
428.20	Si-O-Al stretching	illite	[14]
474.49	Si-O-Al stretching	illite	[15]
532.35	Si-Ostr. Si-O-Al str	Quartz/kaolinite	[14]
694.37	Si-O- stretching	kaolinite	[14]
752.24	Si-O-Al vibration	illite	[16]
779.24	Si-O	quartz	[16]
798.53	OH stretching	kaolinite	[17]
914.26	Al-OH bending	illite	[18]
1033.85	(Si-O-Si, Si-O) Stretching	Illite/kaolinite	[19]
1392.61	Al-O out-of-plane	illite	[16]
1635.64	OH stretching	kaolinite	[17]
2380.16	C=O	carbonate	[20]
3421.72	OH stretching	water	[12]
3552.88	OH stretching	OH interne	[15]
3622.32	OH stretching	kaolinite	[16]
3695.61	OH stretching	kaolinite	[16]

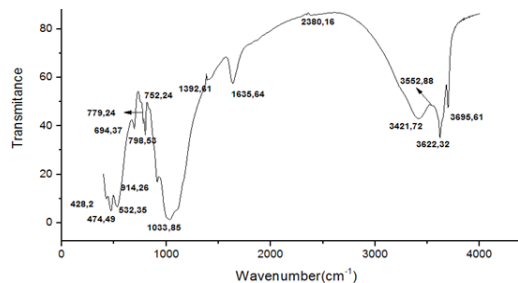


Fig. 3. FTIR spectrum of studied clay.

3.2. BET Surface Area and BJH Pore Size/Volume

BET is an extension of the Langmuir treatment for multi-layer adsorption on a flat and homogeneous surface, and it is important that solid-gas systems are related to condensation [21].

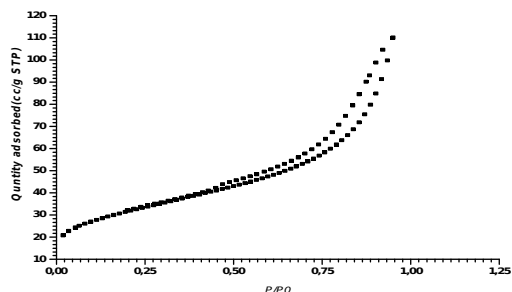
From the curve shape shown in Fig. 4 it can be verified that the isotherm is of type IV however, Fig. 5 showed that the studied clay is mainly a medium pore material. The BET surface area is 110.7064 m²/g. It is accepted that the desorption isotherm is more appropriate than the adsorption isotherm for determining the pore size distribution of an adsorbent.

The surface characteristics of the studied material are given in Table 3, and the pore size is 76.712 Å and the pore volume is 0.152186 cc/g, this value is taken from the cumulative desorption of BJH from Table 3. The distribution of the pore size of the clay studied in Figure 5 shows that the whole studied clays are of the mesoporous type and that the average size of nanoparticles is 541.974 Å.

Table 3:

Surface properties of the natural clay

Parameter	Surface area (m ² /g)	Pore volume (cc/g)	Pore size (Å)
BET Surface Area	110.7064	/	/
Langmuir Surface Area	170.2894	/	/
BJH cumulative adsorption	72.061	0.150018	83.273
BJH cumulative desorption	79.3551	0.152186	76.712



g. 4. Nitrogen adsorption isotherm for EI-Oued Clay

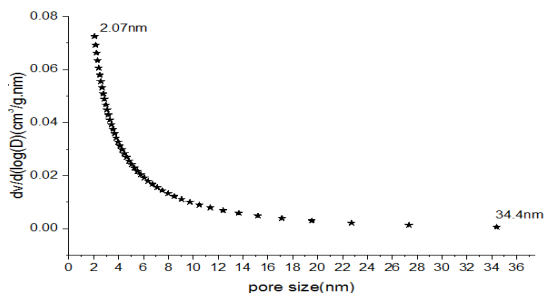


Fig. 5. Pore size distribution of EI-Oued Clay

3.3. SEM/EDS characterization

The Fig. 6 shows clusters of different sizes and dimensions with rough and irregular edges. The clusters vary in size at a scale of fewer than 2 microns. Table 4 and Fig. 7 show the EDS analysis of elemental chemical composition. The analysis shows the actual percentages of the various elements contained in the clay. The table shows percentages of 52.4, 15.3 and 8.9% respectively of O, Si and Al respectively. The lowest amounts are of Na and P. The EDS analysis revealed very reasonable similarities in results with XRD.

The image also shows particles with small dimensions smaller than a micrometer and predominant in the image. Small-sized kaolinite platelets less than 2 μm associated with large particles i.e. large than 10 μm appear. Moreover, the sample contains some of the organic compounds that we discover through the dark areas shown in the picture. The kaolinite may be poorly crystalline due to the presence of impurities. Several authors have found that impurity elements and also illite decrease the whiteness of kaolinites [22-25].

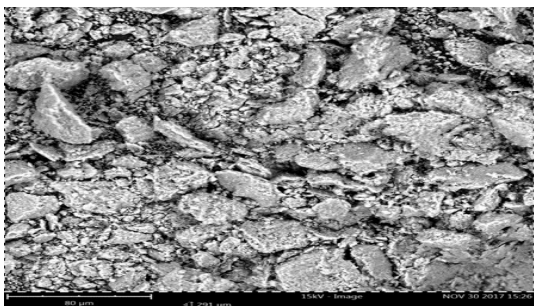


Fig. 6. SEM image of local clay

Table 4.

EDS analysis of elemental chemical composition

Element Symbol	Weight Concentration(%)	Error
Si	15.3	0.2
O	52.4	0.2
Al	8.9	0.1
Fe	5.9	0.3
Mg	1.8	0.7
K	1.6	0.3
Ca	1.2	1.0
N	6.4	1.2
P	0.6	1.7
Na	0.9	0.9
C	4.9	0.4

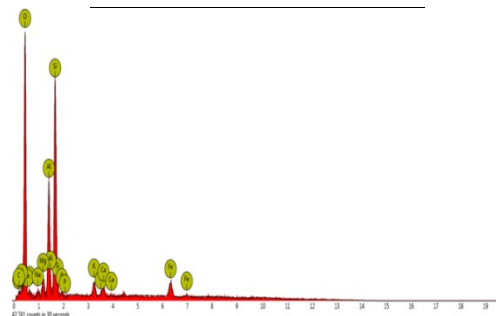


Fig. 7. EDS Spectrum pattern of studied clay

3.4. Cation exchange capacity(CEC)

The experimental protocol and the equation that allows the calculation of CEC have been described previously in section 2.7. Calculated CEC is 20.416 mmol/100g.

4. Conclusion

This work is aimed to determine the mineral properties of natural clay at Saharan zone located southwest of Algeria. Through our study of the purified natural clay, its mineral structure and its physicochemical properties using different analytical methods were determined. It was found that the clay contained mostly the illite with the presence of kaolinite and a minor quantity of quartz using RDX and FTIR as complementary studies. However, BET analysis reveals that the studied clay is mesoporous and it has an isotherm type IV. While its surface area is 110.7064 m^2/g and its pore size and pore volumes are 0.152186 cm^3/g and 76.712 \AA respectively, the average particle size is 541.974 \AA .

Declaration of Competing Interest

The authors declare that they have no known competing financial interests or personal relationships that could have appeared to influence the work reported in this paper.

Acknowledgments

We thank the anonymous reviewers for their careful reading of our study and their many constructive comments and suggestions

Funding

The author(s) received no financial support for the research, authorship, and/or publication of this article.

References

- [1] K.Fukushi, H.Sakai, T.Itono, A.Tamura, S. Arai (2014) Desorption of Intrinsic Cesium from Smectite: Inhibitive Effects of Clay Particle Organization on Cesium Desorption. *Environmental Science Technology*,48, 10743-10749.
- [2]M.Markov, V.Levine, A.Mousatov, E. Kazatchenko (2005) Elastic properties of double-porosity rocks using the differential effective medium model, *Geophysical Prospecting*, 53, 733–754.
- [3] M.Erdemoğlu, S.Erdemoğlu, F.Sayilkan, M. Akarsud, S. Sener, H.Sayilkan (2004) Organo-functional modified pyrophyllite: preparation, characterisation and Pb(II) ion adsorption property. *Applied Clay Science*, 27, 41-52.
- [4]B.B.Velde, A. Meunier (2008) Part of the solution to environmental degradation-the book aids our understanding of mineral formation, *The Origin of Clay Minerals in Soils and Weathered Rocks*, first edition, Springer, Amsterdam.
- [5]L.Sun, C. G.Tian, M.T.Li, X. Y.Meng, L.Wang, R. H.Wang, J. Yin,H.G. Fu (2013) From coconut shell to porous graphene-like nanosheets for high-power supercapacitors, *Journal of Materials Chemistry A*, 1, 6462– 6470.
- [6]A.B.Morgan and J.W.Gilman (2003) Characterization of polymer-layered silicate (clay) nanocomposites by transmission electron microscopy and X-ray diffraction: A comparative study, *Journal of Applied Polymer Science*, 87, 1329-38
- [7]F.Bergaya, B.K.G.Theng,G.Lagaly (2006) General introduction: clays, clay minerals, and clay science, *Handbook of Clay Science*, First Edition. Elsevier,1,1-18.
- [8]Y.L. Liu, H.W. Walker, J.J. Lenhart (2019) Adsorption of microcystin-LR onto kaolinite, illite and montmorillonite, *Chemosphere*, 220, 696–705.
- [9]G. Dirk (2007) Techniques to measure grain-size distributions of loamy sediments: a comparative study of ten instruments for wet analysis, *Sedimentology*,55, 65–96.
- [10]F.Rees, M. O.Simonnot, J. L. Morel (2013) Short-term effects of biochar on soil heavy metal mobility are controlled by intra-particle diffusion and soil pH increase, *European Journal of Soil Science*, 65, 149–161.
- [11]A. F. Gualtieri (2000) Accuracy of XRPD QPA using the combined Rietveld-RIR method, *Journal of Applied Crystallography*, 33, 267-278.
- [12]M.Jana, K. Peter (2001) Baseline Studies of the Clay Minerals Society Source Clays: Infrared Methods, *Clays and Clay Minerals*, 49, 410-432.
- [13]R. M.Hazen, L.W.Finger, R. J.Hemley, H. K.Mao (1989) High-pressure crystal chemistry and amorphization of α -quartz *Solid State Communications*, 72, 507-511.
- [14]A. H.Dewan, S.Mustafi, M.Ahsan, M. S. Ullah (2014) Investigation on physical properties of patia clay (Chittagong), Bangladesh, Bangladesh, *Journal of scientific and industrial research*, 49, 255-262.
- [15]Yen-Ling Liu, Harold W. Walker, John J. Lenhart (2019) The effect of natural organic matter on the adsorption of microcystin-LR onto clay minerals, *Colloid Surf. A-Physicochem. Eng. Asp* , 583,123964.
- [16] S.N.reeti, B. K.Singh (2007) Instrumental characterization of clay by XRF, XRD and FTIR, *Bulletin of Materials Science*, 30 , 235-238.
- [17]Achyut K. Pandaa,b, B.G. Mishraa, D.K. Mishrac, R.K. Singha (2010) Effect of sulphuric acid treatment on the physico-chemical characteristics of kaolin clay, *Colloid Surf. A-Physicochem. Eng. Asp*, 363(1),98-104.
- [18]D. Atia, A.A.Bebba, L. Haddad, A. Zobeidi (2018) Elimination of organic pollutants from urban wastewater by illite-kaolinite local clay from south-east of Algeria, *Ciência e Técnica Vitivinícola*, 33(7), 17-28
- [19]S.Kang, B. Xing (2007) Adsorption of Dicarboxylic Acids by Clay Minerals as Examined by in Situ ATR-FTIR and ex Situ DRIFT, *Langmuir*, 23, 7024-7031.
- [20]B.Suna, G. Elif (2009) Pore structure and surface acidity evaluation of Fe-PILCs, *Turkish Journal of Chemistry*,33, 843–856.
- [21]M. Terashima, M. Fukushima, S. Tanaka (2004) Influence of pH on the surface activity of humic acid: micelle-like aggregate formation and interfacial adsorption, *Colloid Surf. A-Physicochem.Eng. Asp*. 247 (1–3), 77–83.
- [22]S. Chandrasekhar, S. Ramaswamy (2002) Influence of mineral impurities on the properties of kaolin and its thermally treated products, *Applied Clay Science*,21,133–142.
- [23]P. A. Schroeder, N. D. Melear, R. J. Pruett (2003) Quantitative Analysis of Anatase in Georgia Kaolin Using Raman Spectroscopy. *Applied Clay Science*, 23(5-6), pp.299–308.

[24]R. Divakaran, V. N. Sivasankara Pillai (2004) Mechanism of Kaolinite and Titanium Dioxide Flocculation Using Chitosan-Assistance by Fulvic Acids, *Water Research*, 38(8), pp.2135–2143.

[25]P. Raghavan, S. Chandrasekhar, V. Vogt, E. Gock (2004) Separation of titaniferous impurities from kaolin by high shear pretreatment and froth flotation, *Applied Clay Science*, 25(1-2), pp.111–120.